npj | climate and atmospheric science

Article

Published in partnership with CECCR at King Abdulaziz University

https://doi.org/10.1038/s41612-025-00958-5

Carbon uptake of an urban green space inferred from carbonyl sulfide fluxes

Jesse Soininen[1] ✉, Kukka-Maaria Kohonen[2], Pekka Rantala[1], Liisa Kulmala[3], Hermanni Aaltonen[3] & Leena Järvi[1,4]

With several cities worldwide pursuing carbon neutrality in the upcoming decades, there is an increasing interest in quantifying cities' anthropogenic carbon emissions using atmospheric observations. The challenge with both in-situ and remote sensing methods is, however, that the observations include both anthropogenic and biogenic signals. To reduce uncertainties in anthropogenic emission estimations, it is critical to partition biogenic fluxes of carbon dioxide (CO_2) from the observed data. In this study, we, for the first time, examine the suitability of carbonyl sulfide (COS), a proxy for photosynthesis, on partitioning biogenic CO_2 uptake from the ecosystem exchange measured with the eddy covariance (EC) technique over an urban area in Helsinki, Finland. The urban vegetation acts as a clear sink for COS whereas anthropogenic processes show minimal COS emissions within the source area of the measured net carbon flux. We show that two different COS flux-based methods are able to produce the dynamics of photosynthesis by an independent light-response curve-based estimation. Together with commonly used soil and vegetation respiration proxy, we removed biogenic signals from the urban net CO_2 exchange and demonstrated that together with CO_2 fluxes, COS flux can successfully be used to get realistic estimations of anthropogenic carbon emissions using the EC method.

As a consequence of climate change, cities seek ways to carbon neutrality. In order to verify carbon emission reductions, atmospheric measurements are crucial. Measurements of greenhouse gas concentrations and emissions can be made with many different methodologies and in a variety of scales extending from local-scale eddy covariance (EC) measurements[1,2] to city-level tall tower and total column measurements[3–5]. From the different observational methods, EC is the most direct technique to quantify urban emissions by providing the carbon dioxide (CO_2) net exchange (NEE) between a land area and the atmosphere almost continuously. However, partitioning NEE into different flux components is critical to quantifying the anthropogenic emissions and for a comprehensive understanding of the contribution of urban areas to climate change. One of these components is the carbon assimilation, i.e., gross primary production (GPP) of urban vegetation, which takes up part of anthropogenic emissions and thus obscures emission signals[6]. In the absence of anthropogenic emissions GPP can be estimated by subtracting ecosystem scale respiration (R) and NEE (see GPP_{EC} in Eq. (7)). In a human-influenced context, however, CO_2 emissions cannot be neglected, but they reveal a pitfall of the simple GPP_{EC} methodology: It cannot recognize which NEE data have been influenced by anthropogenic CO_2 emissions, and thus cannot be used in an urban context. Consequently, measurements of urban GPP have been residual estimations[7] or are based on light-response curves[8], but direct observations have been missing.

Carbonyl sulfide (COS) is a gaseous compound naturally found in the atmosphere, with an average mixing ratio between 440 and 500 ppt[9] (10^{-12} mol COS per mol dry air). COS is taken up by the plants through their stomata, and its exchange is closely related to the stomatal conductance of vegetation[10]. However, as COS shares the same entrance pathway to the leaf with CO_2, a connection between biogenic COS uptake and GPP can be created[11]. COS is destroyed at the chloroplast surface by the enzyme carbonic anhydrase (CA) in a hydrolysis reaction, and unlike CO_2, is not respired back to the atmosphere as a part of plant metabolism[10]. GPP has been estimated from COS fluxes on vegetated environments[12–14], but its potential has not been harnessed in human-influenced environments. Urban EC fluxes of COS have been studied before over a few weeks in Innsbruck[15], where the main conclusion was that better information on anthropogenic sources is still needed to properly utilize COS as a proxy for GPP in this highly built source area. The same conclusion was obtained by

[1]Institute for Atmospheric and Earth System Research (INAR)/Physics, University of Helsinki, 00014 Helsinki, Finland. [2]Department of Environmental Systems Science, ETH Zürich, 8092 Zürich, Switzerland. [3]Finnish Meteorological Institute, PO Box 503, 00101 Helsinki, Finland. [4]Helsinki Institute of Sustainability Science, University of Helsinki, 00014 Helsinki, Finland. ✉e-mail: jesse.soininen@helsinki.fi

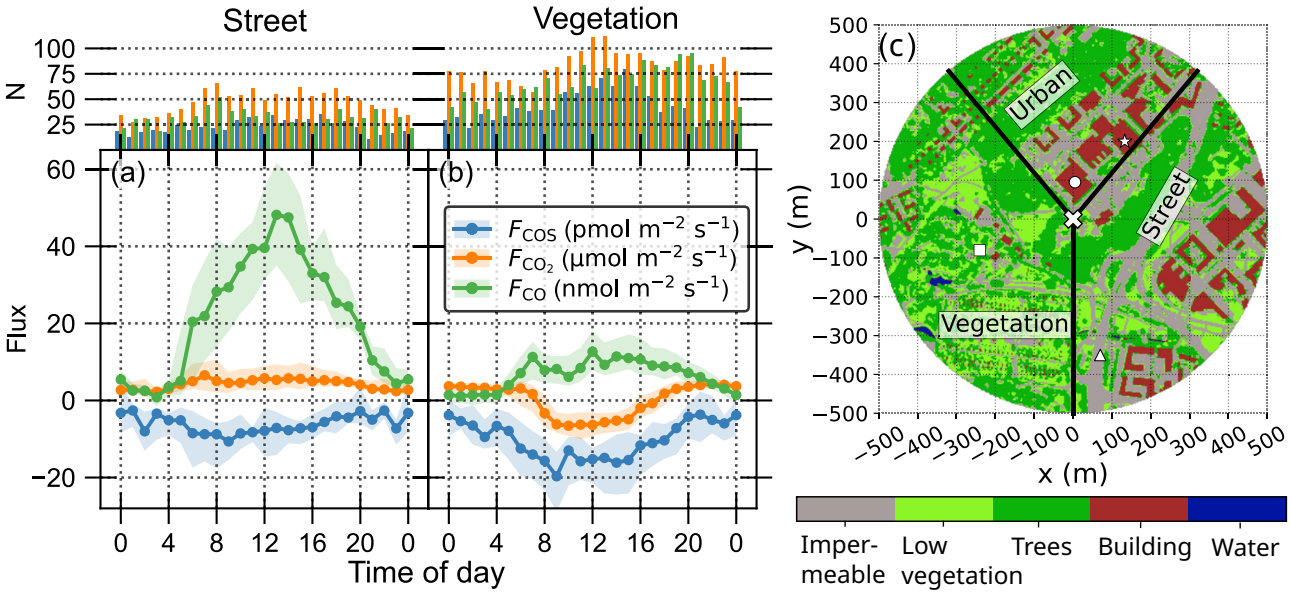

Fig. 1 | Diurnal COS, CO, and CO_2 fluxes measured between May 12 and October 31, 2023 on a street and b vegetation sectors. The top panels show the number (N) of available quality-checked flux data for each gas every hour of the day. Dotted lines in **a** and (**b**) show the median diurnal fluxes and the shadowed areas indicate interquartile ranges of the fluxes. Each flux magnitude is shown on the same y-axis, but the units are different, as indicated in the legend. Panel (**c**) shows the land use around the EC tower, see more details in Fig. S1.

two recent flask sampling studies conducted in Barcelona, Spain[16] and Lutjewad, the Netherlands[17]. They observed notable influence from maritime and industrial sources of COS preventing making solid estimation of GPP.

In this study, we report the first EC fluxes of COS measured over a full growing season in Helsinki, Finland, in an urban area that also has a significant vegetated cover fraction (Figs. 1c, S1, and Table S1). This allows us to examine both biogenic and human-influenced trace gas fluxes in a setting that narrows the gap between the fully vegetated and the heavily built areas studied before. We study the impact of anthropogenic activities in the study area by comparing COS and CO_2 fluxes with carbon monoxide (CO) fluxes, which have been used as an indicator of anthropogenic emissions of CO_2 from combustion processes[1]. We show how COS fluxes can be used to derive urban GPP using two different approaches and use it to calculate anthropogenic CO_2 emissions from NEE.

Results and discussion

Trace gas fluxes during growing period

CO, COS, and CO_2 fluxes in street and vegetation sectors display notable deviations as a consequence of different surface cover fractions and human activities (Figs. 1 and S2). Both sectors function as sinks of COS reaching the highest hourly median uptakes of −10.6 and −19.7 pmol m^{-2} s^{-1}, respectively. To compare, the mean daytime uptake of −23.5 pmol m^{-2} s^{-1} was observed in a deciduous forest during June, August, and September[18], whereas the daily maximum uptake varied between −24 and −33 pmol m^{-2} s^{-1} during different years in a boreal coniferous forest[19]. When the sectors are examined together, a clear positive correlation between COS and CO_2 fluxes is observed, with an uptake ratio of 0.86 pmol μmol^{-1} ($R^2 = 0.39$; Fig. S3a). When only times with simultaneous COS and CO_2 uptake are considered and placed on a similar scatter, the uptake ratio becomes 1.67 pmol μmol^{-1} ($R^2 = 0.52$; not shown). This closely agrees with earlier reported values from leaf chamber measurements in a controlled greenhouse environment, where the ratio was 1.41 pmol μmol^{-1} [11]. This shows the applicability for estimating GPP from COS fluxes at our site, since the methodology relies on the simultaneous uptake of both gases (Eq. (3)).

The street sector is a source of CO_2 with diurnal median values varying between 2.3 and 6.5 μmol m^{-2} s^{-1}. The vegetation sector is on median a CO_2 sink between 8 a.m. and 5 p.m. reaching −6.6 μmol m^{-2} s^{-1}, consistent with previously reported estimates (ca. −7.7 μmol m^{-2} s^{-1})[20]. Nocturnal CO_2 sources are larger on the vegetation than the street sector likely due to soil and vegetation respiration. However, the daytime uptake in the vegetation sector offsets the nocturnal emissions, which is not the case in the street sector. When summed over a median day of the growing period, the vegetation sector sequestrates −8.0 gCO_2 m^{-2} d^{-1}, comparable with −4.6 gCO_2 m^{-2} d^{-1} observed in Baltimore[8], whereas the street sector emits 392.4 gCO_2 m^{-2} d^{-1}. CO_2 and CO fluxes are also significantly correlated during daytime ($R^2 = 0.74$, $p < 0.001$, Fig. S3b) but not nocturnally. Strong correlation originates mainly from road transportation on the street sector, since there are no other combustion processes taking place in similar scales.

The street sector CO and CO_2 fluxes behave differently than corresponding fluxes in the vegetation sector because of transportation in the source area. The daily median CO source of 23.1 nmol m^{-2} s^{-1} originating from, on average 25,000 daily passing cars is comparable to the lowest observed CO fluxes in central London (16.9 nmol m^{-2} s^{-1})[21]. In the vegetation sector, the median daily emission is 7.5 nmol m^{-2} s^{-1}, which still is higher than would be expected in a fully vegetated environment. A boreal forest emitted up to 1.6 nmol m^{-2} s^{-1} [22], and the highest monthly mean on a grazed grassland was 1.9 nmol m^{-2} s^{-1} [23]. Construction work on a tram line has taken place in the vegetation sector, which can explain large parts of the CO emissions. In addition, there may be some other unknown fossil fuel emissions in the vegetation sector such as local wood burning in the allotment garden or site machinery in the botanical garden. Also, another important access road 800–900 m from the tower, can influence the CO fluxes coming from the direction of the sector particularly at night-time when the atmosphere is stable and the source area extends longer. The impact is, however, not visible on CO_2 and COS fluxes due to the large mass of vegetation separating the road from the EC tower.

The EC measurement of COS flux in Innsbruck showed a day-time source, which was connected to exhaust fumes and tire wear of vehicular transportation[15]. A similar deduction was made in Beijing, where tire wear was conjectured the single largest source of COS during summertime[24]. If an anthropogenic COS source originated from vehicular fuel combustion, a clearer relationship between COS and CO fluxes would have been seen, as is the case with CO_2. There is no statistically significant dependence between

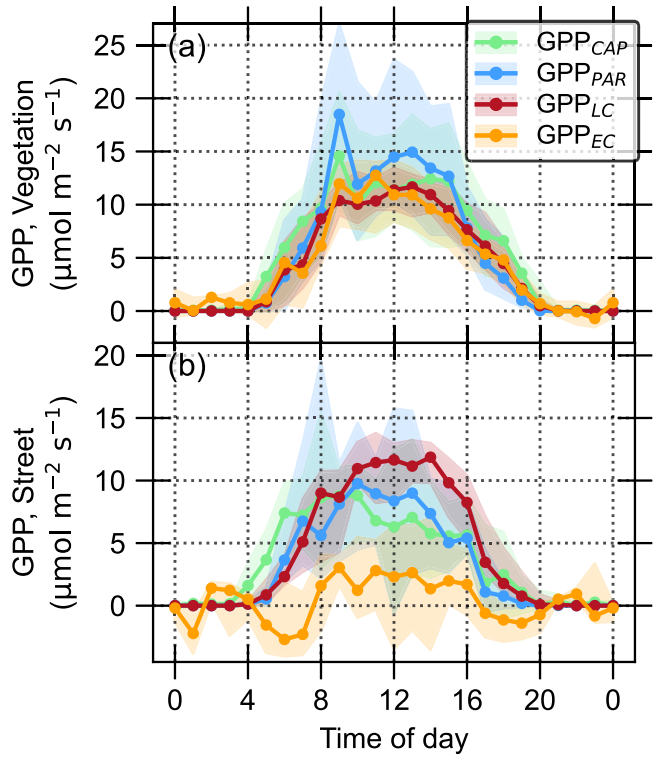

Fig. 2 | Diurnal cycles of gross primary production (GPP) estimated with different methods on the street and vegetation sectors. Panel (**a**) shows the diurnal cycle on the vegetation sector and panel (**b**) shows it on the street sector. Data were collected between May 1 and October 10, 2023. Only moments with data available from all methods were used. Dotted lines show the median diurnal cycle and the shadowed areas in the interquartile range. Note different scales on *y*-axes.

COS and CO fluxes (Fig. S3c) indicating mostly negligible anthropogenic COS emissions. Thus, our results do not support the earlier findings about COS emissions originating from tire wear. However, slight anthropogenic influence cannot be disregarded, particularly in the road sector causing some level of uncertainty in our analyses.

Novel estimation of urban GPP

During the brightest hours (photosynthetically active radiation PAR >700 µmol m^{-2} s^{-1}), the leaf relative uptake (LRU, see the "Methods" section) needed to estimate GPP from COS flux had medians of 1.12 (interquartile range 1.0–1.3) and 1.45 (1.3–1.5) in the vegetation sector, as determined with PAR and CAP methods, respectively. These values compare well with 1.68 obtained for natural ecosystems in a review study[25]. LRU_{PAR} smoothly decreases with PAR, whereas LRU_{CAP} saturates earlier by PAR and has a wider range of values on a single PAR due to the moisture conditions—namely vapor pressure deficit (VPD) and soil water content (SWC)—being taken into account (Fig. S4a).

The four methods used to estimate GPP (GPP_{CAP} and GPP_{PAR} based on COS measurements, GPP_{LC} based on a light-response curve, and GPP_{EC} based on carbon balance partitioning by respiration) provide a similar, qualitatively expected performance on the vegetation sector with the largest uptake in daytime and (near) zero at night-time (Fig. 2a). GPP_{PAR} yields the highest median biogenic uptake of 18.5 µmol m^{-2} s^{-1} whereas with other methods the peak median values remain between 11.7 and 14.6 µmol m^{-2} s^{-1}. GPP_{EC} results in some slightly negative nocturnal GPP values as a consequence of uncertainty in ecosystem respiration (*R*) by the simple model used in this study. The estimated mean *R* (3.9 µmol m^{-2} s^{-1}) agrees with the measurements conducted in Boston metropolitan area[26] [2.6–6.7 µmol m^{-2} s^{-1}], but yield lower values compared to chamber measurements conducted in the vegetation sector in an earlier study[27] [5.5–6.1 µmol m^{-2} s^{-1}]. In the latter, the chamber measurements were only made from lawns and meadows and thus did not present all soil and ground vegetation types within the vegetation sector.

The COS-based GPP estimations match well with GPP_{EC} and GPP_{LC} which are the more traditional methods to estimate GPP from EC measurements in vegetated ecosystems. GPP_{LC} is essentially a parameterization of GPP_{EC} as a function of PAR. Thus, the light response curve estimation of GPP can be used as a reference value for photosynthesis where there is a distinct and well-defined green sector. Also, GPP_{LC} works well against the small and occasional anthropogenic contributions visible in GPP_{EC} due to the averaging nature of parameterization. However, without the near-pure biogenic signal, GPP_{LC} cannot be parameterized, which becomes an essence of the NEE partitioning problem in urban areas.

GPP_{CAP} and GPP_{PAR} provide an independent mean to estimate GPP, but as both rely on COS concentration and flux measurements, they show more variability with similar peaks than the other two methods. GPP_{PAR} reaches higher peak values and shows steeper changes in both morning and evening hours, as PAR is considered the only limiting factor of LRU. On the contrary, GPP_{CAP} considers the environmental water availability as a part of the stomatal conductance model, which makes the slope more gentle during the transition periods of the day. This implies an insufficiency of GPP_{PAR} in the current ecosystem. High GPP values given by the method were noted already when the parameterization was used in a boreal forest site[13] and in comparison with other methods at the same site[14]. High estimates are based on GPP_{PAR} being originally parameterized in optimal light conditions, which translates into unrealistically high GPP. Even though light conditions are less limited on a relatively open urban canopy compared to boreal forest, the method still overestimates. Nevertheless, it is used despite the different imperfections to provide the first COS-based GPP estimates.

Differences between methods are emphasized in the street sector (Fig. 2b), where GPP estimates are lower than in the vegetation sector. As expected, the pitfall of using traditional, CO_2-based partitioning of EC fluxes (GPP_{EC}) in a human-influenced context becomes apparent. Because the method only assumes a temperature-dependent *R* and GPP to play a role, it fails to recognize moments with negative GPP as anthropogenically influenced. Hence, it is not reasonable to use it as a reference for other models' performance. The other methods yield qualitatively reasonable patterns for CO_2 uptake. The magnitude of the estimated GPP follows inversely the number of environmental variables used in each method: GPP_{LC} depends on PAR and yields a median GPP peak of 11.9 µmol m^{-2} s^{-1}, GPP_{PAR} additionally depends on COS flux and ratio of CO_2 and COS molar fraction (X_{CO_2}/X_{COS}) resulting a peak value of 9.7 µmol m^{-2} s^{-1}, and GPP_{CAP} with most environmental dependencies resulting a peak value of 8.8 µmol m^{-2} s^{-1}. GPP_{CAP} shows an earlier morning increase due to a more flexible response to environmental variables. Both COS-based methods decrease earlier than GPP_{LC} in the afternoon, with GPP_{CAP} being 50% of GPP_{LC} between 11 a.m. and 5 p.m. This is partly caused by the diurnal cycle of COS flux (Fig. 1a) and partly by the variability of X_{CO_2}/X_{COS}, which is approximately 10% lower in the afternoon than in the morning (Fig. S5c).

Uncertainties

The benefit of the COS-based methods is that real-time information on the plant uptake is obtained in the form of COS flux. This, however, assumes that the measured COS signal contains only the biogenic impact, which is an ideal case. Soil is also a known contributor to the ecosystem scale COS fluxes. Soil fluxes were not separately measured in this study, but have earlier been deemed to account for 10–20% of the ecosystem scale COS uptake in a boreal pine forest[28]. Overall, soils with oxygen mostly function as moderate COS sinks, with the exceptions of deserts and some agricultural lands[25,29]. Due to the small contribution of soils to net COS flux, we ignore it and consider it as an uncertainty.

For COS measurements made in a more densely built environment, a combination with modeling may be needed because the signal of biogenic uptake gets easily mixed with the anthropogenic signal. The possible traces of exhaustion fumes can dilute the biogenic signal, for which reason COS methodology is potentially jeopardized in cities. For example, a flask

sampling over the San Francisco Bay Area concluded that improved GPP estimates are needed to distinguish urban biosphere signals[30], whereas another flask sampling study in Barcelona could distinguish a sink of COS in the urban forests, but not anymore in individual parks in the densely built parts of city[16]. Overall, for the COS-based methods to work in CO_2 flux partitioning, a sufficient amount of photosynthesizing biomass is needed in the flux source area. We show that on the street sector, which has a 45% vegetated land cover fraction, COS-based GPP yields sensible results. Still, this is not necessarily the lower limit for the minimum required vegetation for observing COS signals.

The path from COS flux to GPP is paved through LRU, which is directly related to stomatal conductance instead of GPP but is easier to utilize than a complex model for vegetative uptake of CO_2. Moreover, combining LRU with measurements is simpler than a model for stomatal conductance. LRU is not a rainmaker, however, as simplicity comes with a price. When studying our heterogeneous environment, it is not possible to consider the variability in species composition, light and moisture conditions, and soil properties, which are known to impact LRU[13,31]. Instead, a heterogeneous environment forces us to make assumptions related to the urban environment overall. As it cannot be distinguished how different vegetation types impact the measured signal within and between the sectors, the fluxes contain the impact of diverse vegetation on the ecosystem level. This sets an unknown level of uncertainty in the analysis. LRU methodology will, however, be useful, because the street and the vegetation sectors experience different atmospheric mixing ratios of COS (Fig. S5), which is related to the GPP estimated using LRU. In this study, two parameterizations of LRU are used, both of which have been derived for a boreal forest site (see GPP methods). Even though using LRU_{PAR} and LRU_{CAP} is justified as LRU has been found to be relatively invariant within the boreal biome[32], it is important to note that LRU values between species may vary notably[33]. The LRU values we have obtained should be used with care in other urban areas as they are only representative of the boreal biome. A Monte Carlo-based uncertainty analysis conducted showed, however, that the accuracy of COS measurements is a greater source of uncertainty than the LRU parameterizations (see SI Uncertainty analysis).

The Kok effect, or the light-induced part of the respiration[34] has not been considered when parameterizing GPP_{LC} and R. The possible uncertainty caused by this has been studied using Monte Carlo simulation (see SI Uncertainty analysis), which shows that R estimate has most error around the lightest time of the year (Fig. S6e), which was also notably warm and dry in Helsinki. Thus, the uncertainty may derive from a low nocturnal data availability affecting parameterization, or R being impacted by the dry conditions. Over the measurement period, the cumulative uncertainty of R is 1.7%. To GPP_{LC} this is reflected as a 0.9% uncertainty, with similar behavior over the measurement period.

Residually solved anthropogenic emissions

The anthropogenic CO_2 fluxes (F_a) in the street sector obtained with CAP, PAR, and LC methods using Eq. (1) correlate with a bottom-up estimate of CO_2 emissions from traffic ($F_{CO_{2,traffic}}$) but show slightly lower emissions (Fig. 3). $F_{CO_{2,traffic}}$ reaches a median of 10.2 μmol m^{-2} s^{-1} whereas the other methods range between 8.2 and 9.2 μmol m^{-2} s^{-1}. An earlier modeling study reported a summer-time maximum traffic emission of 9.3 μmol m^{-2} s^{-1} [35], which is close to our estimates. A notable feature of all methods is the underestimation of nocturnal emissions, which derives from uncertainty in the ecosystem scale respiration estimate. Difference between F_a's and $F_{CO_{2,traffic}}$ partly results from the different natures of methodologies compared. EC can only observe one limited footprint area at a time, whereas the bottom-up estimate contains the full emission without any going undetected or taken up by the vegetation on the way to the EC tower. In principle, $F_{CO_{2,traffic}}$ assumes the full traffic signal to arrive at the EC setup every moment. $F_{a,LC}$ is closest to the bottom-up estimates (R^2 = 0.83, Fig. 3), which is the only of the three methods showing the expected two peaks on F_a by morning and afternoon rush hours. $F_{a,LC}$ shows, on average, 33% lower values when compared to $F_{CO_{2,traffic}}$. A close fit confirms the assumption of similarly behaving vegetation between the two sectors since GPP_{LC} parameterized on the vegetation sector performs well on the street sector. Although the best results are obtained with GPP_{LC}, it is not reproducible in every urban setting, as a large vegetative mass without notable anthropogenic CO_2 emissions is required for its parameterization.

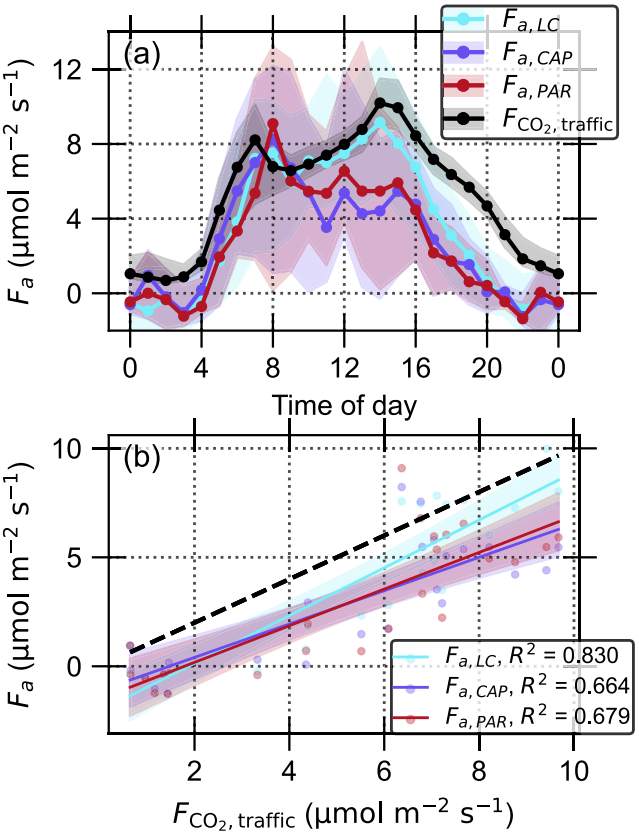

Fig. 3 | Estimates of the anthropogenic CO_2 fluxes (F_a) in the street sector. **a** Median diurnal cycle obtained with different methods (LC, CAP, PAR) and an independent bottom-up fossil fuel estimate ($F_{CO_{2,traffic}}$). Shadowed areas indicate the interquartile ranges. **b** Comparison of half-hourly estimates by different methods against ($F_{CO_{2,traffic}}$). The solid lines show the fits, shaded area the 95% confidence intervals, and the dashed line 1:1 ratio.

The COS-based CAP and PAR methods have R^2 values of 0.66 and 0.68, respectively. The lower GPP values during the afternoon hours (Fig. 2) when compared to GPP_{LC} translates into lower afternoon F_a as it is obtained as a residual from GPP and R. An additive part of the discrepancy can derive from the accumulation of error: Initial signal of high-frequency X_{COS} measurements has a lot of noise by default, which affects the quality of the flux calculated with the EC technique. The random errors of CO_2 fluxes can vary between 10–30%[36] but are even 35% for COS fluxes[37]. Looking at the big picture, however, COS methods succeed qualitatively in producing diurnal dynamics of F_a and a relatively good correlation, which is encouraging. If $F_{a,LC}$ is considered the desired output, then CAP and PAR both produce credible results, even though the daily sums of emissions for $F_{a,PAR}$ and $F_{a,CAP}$ are 24% and 21% lower than that of $F_{a,LC}$, respectively.

Long-term variability

All methods catch the variability of the anthropogenic (traffic in our case) CO_2 emissions and GPP during the measurement period (Fig. 4). $F_{CO_{2,traffic}}$ in the street sector, it varies little over the measurement period, remaining between 6.9 and 8.4 μmol m^{-2} s^{-1}. As with the diurnal variability, F_a obtained with different methods yields mostly lower estimates than obtained with the bottom-up approach. $F_{a,LC}$ is, on average, the closest to $F_{CO_{2,traffic}}$ (3.1–10.9 μmol m^{-2} s^{-1}), while COS based methods yield mostly

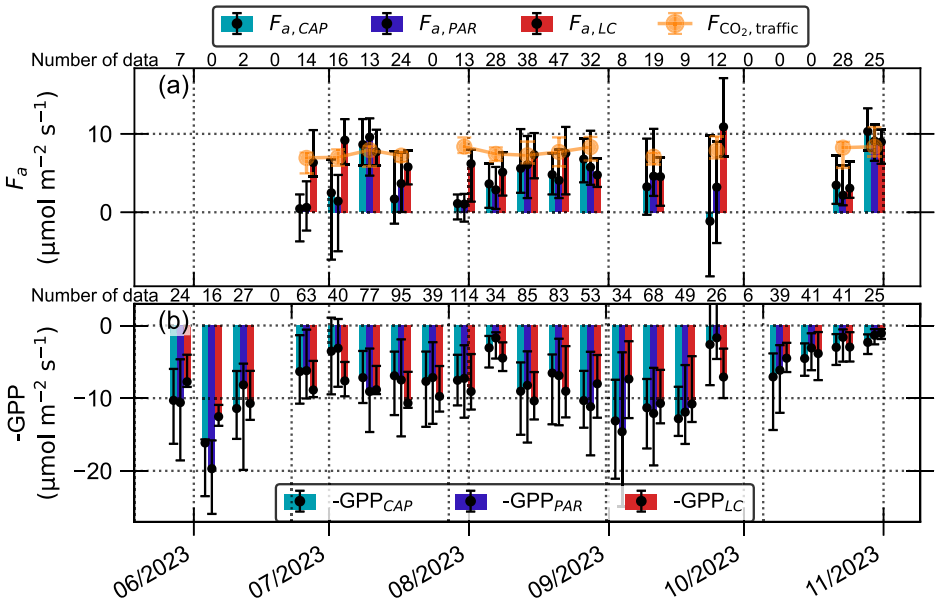

Fig. 4 | Temporal evolution of the estimated anthropogenic CO_2 fluxes (F_a) and gross primary productivity (GPP) in the street and vegetation sectors using different methods. Panel (**a**) shows F_a at the street sector and panel (**b**) shows GPP from both the vegetation and the street sectors. Nighttime data (PAR < 10 μmol m^{-2} s^{-1}) are omitted. Bins show the median value from 10-day periods, and the whiskers indicate the interquartile range. Orange data with error bars on panel (**a**) show the median and interquartile range of the bottom-up estimate of fossil fuel emissions on the street sector. It is generalized into the vegetation sector by normalizing values according to the paved land surface area. The number of accepted data points for each group of bins is shown on top of the panels, and only those times with more than 10 points were plotted.

notably lower estimates ($F_{a,CAP}$: −1.1 to 10.3 μmol m^{-2} s^{-1}, $F_{a,PAR}$: 0.6–9.6 μmol m^{-2} s^{-1}). Performance of COS-based methods improves notably when the amount of available data from street sector increases. Part of $F_{a,LC}$'s success comes from the fact that parameterizations always ignore a significant amount of variability, which is detected in the COS flux-based methodology. However, the results encourage the use of light response curves where applicable.

The seasonal dynamics of GPP (Fig. 4b) reflect variations in environmental conditions that the different methods are able to catch. After the driest and hottest period at the end of June (Fig. S7), there is a clear dip in the magnitude of GPP. The cloudy and rainy start of August shows a clear decrease in biogenic activity. During October, the vegetation prepares for winter dormancy, and the photosynthesis ceases completely. Finally, different methods converge towards each other: GPP approaches zero regardless of the method, thus F_a approaches R—NEE. The last week of the campaign shows an increase in all F_a's without a significant increase in data availability. This suggests that as the temperatures fall closer to 0 °C, it becomes more likely that there are anthropogenic CO_2 emissions from also other than vehicular sources. GPP_{LC}, the most accurate on F_a, shows the least variability with the average observed CO_2 uptake of 7.9 μmol m^{-2} s^{-1}. COS flux-based methods are, as expected, similar to each other, but GPP_{PAR} shows larger variability both between and within the weeks. GPP_{CAP} yields the lowest average CO_2 uptake, but a relatively high reactivity to the environmental conditions, shown as a higher standard deviation than GPP_{LC}.

In summary, we demonstrated that COS fluxes can be used to give realistic measurement-based estimates of urban ecosystem level GPP both on diurnal and season scales. The obtained GPP values can be used together with the estimation of ecosystem respiration to estimate anthropogenic emissions within the source area of the EC measurements. Compared to light-response curves COS-based methods need a lower fraction of green area and are not dependent on an NEE measurement of purely biogenic origin, thus being a better fit for the urban environment. Nonetheless, the light-response curve of GPP remains a useful and more accurate tool in the areas where a reasonable parameterization is possible. We also acknowledge that the COS methodology might not be applicable in environments with high anthropogenic influence. However, in the areas, where the fraction of vegetated areas is large, COS flux measurements can provide useful insights to estimate the magnitude of CO_2 uptake within the footprint.

Future research on urban COS exchange should consider conducting EC and chamber measurements using both shoot and soil chambers in urban vegetation to obtain a more detailed picture of the COS and CO_2 fluxes along the ecosystem scale. Furthermore, COS-based GPP methodologies should be compared with other methodologies, such as remote-sensed solar-induced chlorophyll fluorescence (SIF). By expanding the methodology to other urban areas also the global COS budget closure could be further enhanced.

Methods

Measurement setup

Eddy covariance (EC) measurements were conducted on top of a 31 m high measurement tower located at the SMEAR III (Station for Measuring Ecosystem–Atmosphere Relationships[38]) in Helsinki, Finland (60°12'N, 24°58'E, 26 m above sea level). The station serves as an ICOS ecosystem associate site (FI-Kmp). The continuous measurement setup consisted of a uSonic-3 Scientific sonic anemometer (Metek GmbH, Elmshorn, Germany) to measure three-dimensional wind components and an enclosed path infrared gas analyzer (LI-7200RS, LI-COR, Lincoln, NE, USA), the standardized device for ICOS to measure CO_2 and water vapor molar fractions[39]. These continuous measurements were complemented with an Aerodyne QCL gas analyzer (AD-QCL; Aerodyne Research Inc., Billerica, MA, USA) between 12 May and 31 October 2023 to measure the molar fractions of CO, COS, CO_2, and water vapor. Sample air was drawn to the base of the tower through a 40 m long PTFE tubing (8 mm i.d., 22 l min^{-1}), from where a subflow of 7.5 l min^{-1} was guided to the instrument through 4 m long PTFE tubing (4 mm i.d.) All measurements were made at 10 Hz frequency. COS concentration was calibrated daily against the NOAA-2004 scale (474.2 ppt) every 24 h. The device's drift was corrected by employing nitrogen as a background measurement every three hours. Auxiliary environmental measurements are described in Supporting Information (SI).

Flux processing

The vertical wind and trace gas molar fractions were utilized to compute 30-min average fluxes. The process involved despiking, linear detrending and 2-dimensional coordinate rotation, following standard EC processing approaches[40,41]. The fluxes were computed utilizing the maximum covariance method where the time lag of CO_2 was used for COS due to the noisy COS signal[37]. The obtained fluxes underwent spectral and storage corrections, which are described in SI. The co-spectra of COS with vertical wind exhibited a distinctive shape for the highest frequencies (Fig. S8), and the spectral correction of CO_2 was thus utilized. Storage flux below the measurement height was derived by assuming a uniform concentration change

through the profile for each gas (Fig. S9)[37,42–44]. To ensure the quality of the flux data, the following criteria were applied: flux stationarity <60%, kurtosis of the observation distribution between 1 and 8, and skewness between −2 and 2. Additionally, u_* filtering, with a threshold set at $u_* = 0.19$ m s^{-1}, was employed to eliminate the impact of low-turbulence situations[43]. Quality control was passed by 37.9%, 59.6%, and 45.9% of COS, CO_2, and CO fluxes, respectively. The relatively high omission percentage for COS fluxes was anticipated, primarily attributed to a low signal-to-noise ratio resulting from the inherently low atmospheric molar fraction of COS. Previous studies in forest ecosystems have utilized 34%[18] and 48%[37] of all COS flux data. The time series of fluxes that passed the quality filter are illustrated in Fig. S2. A comparison between AD-QCL and LI-7200 latent heat (LE) and CO_2 fluxes exhibited a good agreement ($R^2 = 0.83$ and $R^2 = 0.69$), with AD-QCL yielding 14% larger and 5.4% smaller flux values, respectively (Fig. S10). Data were not gap-filled due to the heterogeneous nature of the site, and as gap-filling can bring uncertainty to the analysis[45].

Ecosystem-scale urban CO_2 exchange

The footprint area of the EC setup was divided into three sectors (Fig. S1), of which street and vegetation were used in this analysis as the wind direction was seldom from the built sector. The vegetation sector had 80% green land cover, whereas the street sector had almost equal amounts of paved (41%) and vegetated (46%) surfaces (Table S1). The major difference between these two sectors is the amount of human activity. The vegetation sector houses a botanical garden, an allotment garden, and recreational green spaces, while one of the busiest access roads of Helsinki city center passes the street sector. Over the study period, the road had an average traffic count of 23,400 vehicles per day as measured by the City of Helsinki traffic counter located 350 m south of the EC tower.

The urban ecosystem- or local-scale net exchange of CO_2 (NEE, in μmol m^{-2} s^{-1}) as measured using the EC technique can be described using a simplified equation

$$\mathrm{NEE} = F_a + R - \mathrm{GPP}, \tag{1}$$

where R is the combined vegetation and soil respiration, GPP is the amount of photosynthetic uptake of CO_2, and F_a combines all the anthropogenic sources of CO_2 within the footprint area. R can be further divided into autotrophic and heterotrophic respirations, i.e., natural CO_2 release from plants and heterotrophic activity, such as soil microbial decomposition, and the F_a into emissions from human respiration, building heating, and transportation[8]. In the vicinity of SMEAR III, however, transportation is by far the largest anthropogenic CO_2 source, as building emissions take place elsewhere due to district heating, and human respiration is also modest compared to traffic[35]. Thus, F_a is considered synonymous with traffic emissions, keeping in mind the consequent uncertainty. To separate F_a, which is commonly the interest of urban observations, from the other components, estimations for R and GPP are needed.

A commonly used practice is to estimate R using an exponential function on temperature:

$$R = R_C Q_{10}^{T_{sa}/10}, \tag{2}$$

where R_C is the base level of respiration, Q_{10} describes the increase of R when temperature increases by 10 °C, and T_{sa} is the driving temperature of the respiration. Following[14], a half-hourly average of 10 cm soil temperature from the botanical garden and 16 m air temperature from the EC tower was used. Parameters were obtained by fitting night-time (PAR < 10μmol m^{-2} s^{-1}) NEE data from the vegetation sector (Fig. S11), which is a common practice when estimating R on vegetated ecosystems[46]. More information about the parameterization is available in SI.

GPP methods

The photosynthetic carbon uptake of urban green areas was estimated using four different methods, with two relying on COS flux measurements. To estimate GPP from ecosystem-scale fluxes of COS (F_{COS}), a leaf relative uptake (LRU) of COS and CO_2 was used[12,14,47], as follows:

$$\mathrm{GPP}_{COS} = \frac{F_{COS}}{\mathrm{LRU}} \frac{X_{CO_2}}{X_{COS}} \tag{3}$$

where X_{CO_2} and X_{COS} are molar fractions (shown in Fig. S12). In essence, LRU describes the ratio of the COS and CO_2 fluxes normalized with their molar fractions. Originally, LRU was considered as a constant[11,12], but later studies have shown the importance of the diurnal dynamics of LRU[13,14]. Ideally, LRU is measured independently using leaf chamber measurements of COS and CO_2 to get a sturdy estimate for it. However, chamber measurements are often neither feasible nor representative, which presents a challenge, particularly in urban green areas with highly diverse plant species. We tested two different means to parameterize LRU on an ecosystem scale (see below).

GPP_{PAR} from COS flux and light response of LRU. An earlier study made an LRU parameterization based on chamber measurements in Hyytiälä forest station[13]. It represents the LRU of the top canopy of a boreal *Pinus sylvestris* forest as a function of PAR following

$$\mathrm{LRU}_{PAR} = \frac{607.26\,\mu\mathrm{mol\ m^{-2}s^{-1}}}{\mathrm{PAR}} + 0.57. \tag{4}$$

An earlier study observed no significant differences between the LRU values of coniferous and broad-leaved tree species[31]. Furthermore, it has been shown that LRU is relatively invariant within the boreal biome[32]. Hence, the method is used here as an approximation for the diverse footprint area with predominantly broad-leaved trees and managed urban grasslands. LRU_{PAR} was used in (3) to obtain GPP_{PAR} in both the vegetation and street sectors.

GPP_{CAP} from COS flux and environmental parameterization. GPP_{CAP} is based on the CAP (carboxylation capacity) stomatal conductance optimization model[14,48]. Besides PAR, it takes into account more environmental variables relevant for LRU, such as VPD, SWC, and leaf area index (LAI) following

$$\mathrm{LRU}_{CAP} = \frac{1}{1.21} \frac{X_{CO_2}}{X_{CO_2} - \Gamma^*} \left(1 + \sqrt{\frac{K_{sl}|\Psi_c|}{1.6 g_c \mathrm{VPD}}} \sqrt{1 + \frac{2\Gamma^* g_c}{\alpha \mathrm{PAR}}}\right). \tag{5}$$

It is, in principle, universal, although applying it on different sites requires good availability of environmental parameters. The list of variables and parameters and their source is shown in Table S3. LRU_{CAP} is used in Eq. (3) to obtain GPP_{CAP} in both urban and street sectors.

GPP_{LC} from an ecosystem-scale light response curve. GPP_{LC} utilizes a form of saturating light response curve also originally used on forest ecosystems. The formulation was taken from a subarctic boreal forest as[46]

$$\mathrm{GPP}_{LC} = \frac{\alpha \mathrm{PAR} + P_{max} - \sqrt{(\alpha \mathrm{PAR} + P_{max})^2 - 4\theta P_{max} \mathrm{PAR}}}{2\theta} f(T_a), \tag{6}$$

where α is the quantum yield, or the initial slope of the light response curve, I denotes PAR, P_{max} light-saturated rate of GPP, and θ is a curvature parameter. The temperature response of photosynthesis ($f(T_a)$) is taken into account as

$$f(T_a) = \frac{1}{1 + \exp(2(T_0 - T_a))},$$

where T_a is air temperature at 16 m, and $T_0 = -2$ °C is the inflection point. Parameters were fitted as described in SI (Fig. S11). GPP_{LC} was then calculated for both vegetation and road sectors using the fitted parameters.

GPP_{EC} from traditional CO_2 flux partitioning. GPP_{EC} was employed in a "traditional" manner to distinguish carbon exchange components in vegetated ecosystems where it is estimated as a residual from NEE measured using EC and R(2), as follows:

$$GPP_{EC} = R - NEE. \quad (7)$$

In this study, the method was primarily utilized for comparison to the other methods and secondarily to demonstrate its incompatibility in areas where anthropogenic CO_2 emissions become non-negligible.

Traffic emissions

To assess the accuracy of the final anthropogenic emissions obtained with different GPP estimates, we compare the flux-derived estimates against bottom-up estimates of fossil fuel emissions originating from vehicular transportation in the street sector ($F_{CO_2,traffic}$). Estimates of F_a were only made for the street sector because human activities in the vegetation sector were small. Also, we only consider F_a estimates just by LC, CAP, and PAR methods as for EC method F_a is trivially zero. The traffic rate measured at the access road by the City of Helsinki was combined with weighted unit emission factors (EF) obtained from The Handbook of Emission Factors for Road Transport (HBEFA)[49]. *EF*s were obtained separately for different road types, each with their mean velocities matching with those obtained from the traffic counts. Velocity-dependent EF was obtained by fitting a line to the velocity-EF plane (Fig. S13b). The obtained relationship was

$$EF = -0.87V + 182.7 \left[\mathrm{gCO_2\,km^{-1}\,car^{-1}}\right] \quad (8)$$

where V is the average speed in 30-min period in km h^{-1}. The emission factor was multiplied by the number of cars per 30-min period and normalized by the area of paved land cover on the street sector to obtain the final vehicular CO_2 emission. The emission factors on the velocity range from 30 to 70 km h^{-1} were considered trustworthy with this methodology. Earlier modeling from the area in 2012 estimated *EF* of 298 $gCO_2\,km^{-1}\,car^{-1}$ [35], which is considerably higher than ours (183 ± 7 $gCO_2\,km^{-1}\,car^{-1}$). This can be partly accounted for the development of cars and the slowly increasing fraction of electronic vehicles and partly for the different methodologies used.

The real CO_2 signal originating from the street sector gets diluted on its path to the EC setup depending on the prevailing wind direction and the distance to the street. To account for this, an artificial dilution was added to the $F_{CO_2,traffic}$ estimate. This was achieved by dividing the street sector into 20° slices with radii of 350 m (distance to the traffic counter, see Fig. S1), and weighting each estimate with a factor

$$W_{slice} = \frac{p_{slice}}{p_{slice,max}}, \quad (9)$$

where p_{slice} is the paved fraction in each slice and $p_{slice,max}$ is the highest paved fraction across all slices. Thus, $F_{CO_2,traffic}$ was weighted for every timestep with a factor ranging between 0–1 depending on the average wind direction during the 30-min period.

Data availability

The dataset generated and analyzed during the current study are available in a Zenodo repository: https://doi.org/10.5281/zenodo.11928482.

Code availability

The underlying code used to generate and analyze the data during the current study are available in a Zenodo repository: https://doi.org/10.5281/zenodo.11928482.

Received: 26 June 2024; Accepted: 4 February 2025;
Published online: 06 March 2025

References

1. Wu, K. et al. Source decomposition of eddy-covariance CO_2 flux measurements for evaluating a high-resolution urban CO_2 emissions inventory. *Environ. Res. Lett.* **17**, 074035 (2022).
2. Järvi, L. et al. Seasonal and annual variation of carbon dioxide surface fluxes in Helsinki, Finland, in 2006–2010. *Atmos. Chem. Phys.* **12**, 8475–8489 (2012).
3. Lian, J. et al. Can we use atmospheric CO_2 measurements to verify emission trends reported by cities? Lessons from a 6-year atmospheric inversion over Paris. *Atmos. Chem. Phys.* **23**, 8823–8835 (2023).
4. Turnbull, J. C. et al. Synthesis of urban CO_2 emission estimates from multiple methods from the Indianapolis Flux Project (INFLUX). *Environ. Sci. Technol.* **53**, 287–295 (2019).
5. Zhao, X. et al. Analysis of total column CO_2 and CH_4 measurements in Berlin with WRF-GHG. *Atmos. Chem. Phys.* **19**, 11279–11302 (2019).
6. Velasco, E. & Roth, M. Cities as net sources of CO_2: review of atmospheric CO_2 exchange in urban environments measured by eddy covariance technique. *Geogr. Compass* **4**, 1238–1259 (2010).
7. Menzer, O. & McFadden, J. P. Statistical partitioning of a three-year time series of direct urban net CO_2 flux measurements into biogenic and anthropogenic components. *Atmos. Environ.* **170**, 319–333 (2017).
8. Crawford, B., Grimmond, C. S. & Christen, A. Five years of carbon dioxide fluxes measurements in a highly vegetated suburban area. *Atmos. Environ.* **45**, 896–905 (2011).
9. Montzka, S. A. et al. On the global distribution, seasonality, and budget of atmospheric carbonyl sulfide (COS) and some similarities to CO_2. *J. Geophys. Res. Atmos.* **112**, D09302 (2007).
10. Wohlfahrt, G. et al. Carbonyl sulfide (COS) as a tracer for canopy photosynthesis transpiration and stomatal conductance: potential and limitations. *Plant Cell Environ.* **35**, 657–667 (2012).
11. Stimler, K., Montzka, S. A., Berry, J. A., Rudich, Y. & Yakir, D. Relationships between carbonyl sulfide (COS) and CO_2 during leaf gas exchange. *New Phytol.* **186**, 869–878 (2010).
12. Asaf, D. et al. Ecosystem photosynthesis inferred from measurements of carbonyl sulphide flux. *Nat. Geosci.* **6**, 186–190 (2013).
13. Kooijmans, L. M. et al. Influences of light and humidity on carbonyl sulfide-based estimates of photosynthesis. *Proc. Natl Acad. Sci. USA* **116**, 2470–2475 (2019).
14. Kohonen, K.-M. et al. Intercomparison of methods to estimate gross primary production based on CO_2 and COS flux measurements. *Biogeosciences* **19**, 4067–4088 (2022).
15. Karl, T. et al. Studying urban climate and air quality in the Alps. *Bull. Am. Meteorol. Soc.* **101**, E488–E507 (2020).
16. Estruch, C. et al. Exploring the influence of land use on the urban carbonyl sulfide budget: a case study of the metropolitan area of Barcelona. *J. Geophys. Res. Atmos.* **128**, e2023JD039497 (2023).
17. Zanchetta, A. et al. Sources and sinks of carbonyl sulfide inferred from tower and mobile atmospheric observations in the Netherlands. *Biogeosciences* **20**, 3539–3553 (2023).
18. Commane, R. et al. Seasonal fluxes of carbonyl sulfide in a midlatitude forest. *Proc. Natl Acad. Sci. USA* **112**, 14162–14167 (2015).
19. Vesala, T. et al. Long-term fluxes of carbonyl sulfide and their seasonality and interannual variability in a boreal forest. *Atmos. Chem. Phys.* **22**, 2569–2584 (2022).
20. Abadie, C. et al. Carbon and water fluxes of the boreal evergreen needleleaf forest biome constrained by assimilating ecosystem carbonyl sulfide flux observations. *J. Geophys. Res. Biogeosci.* **128**, e2023JG007407 (2023).

21. Helfter, C. et al. Spatial and temporal variability of urban fluxes of methane, carbon monoxide and carbon dioxide above London, UK. *Atmos. Chem. Phys.* **16**, 10543–10557 (2016).
22. Laasonen, A. *Biogenic Carbon Monoxide Fluxes in Four Terrestrial Ecosystems* (University of Helsinki, Helsinki, 2021).
23. Cowan, N. et al. Seasonal fluxes of carbon monoxide from an intensively grazed grassland in Scotland. *Atmos. Environ.* **194**, 170–178 (2018).
24. Cheng, Y. et al. Characteristics and anthropogenic sources of carbonyl sulfide in Beijing. *J. Environ. Sci. (China)* **28**, 163–170 (2015).
25. Whelan, M. E. et al. Reviews and syntheses: carbonyl sulfide as a multi-scale tracer for carbon and water cycles. *Biogeosciences* **15**, 3625–3657 (2018).
26. Decina, S. M. et al. Soil respiration contributes substantially to urban carbon fluxes in the greater Boston area. *Environ. Pollut.* **212**, 433–439 (2016).
27. Karvinen, E., Backman, L., Järvi, L. & Kulmala, L. Soil respiration across a variety of tree-covered urban green spaces in Helsinki, Finland. *SOIL* **10**, 381–406 (2024).
28. Sun, W. et al. Soil fluxes of carbonyl sulfide (COS), carbon monoxide, and carbon dioxide in a boreal forest in southern Finland. *Atmos. Chem. Phys.* **18**, 1363–1378 (2018).
29. Maseyk, K. et al. Sources and sinks of carbonyl sulfide in an agricultural field in the Southern Great Plains. *Proc. Natl Acad. Sci. USA* **111**, 9064–9069 (2014).
30. Villalba, G. et al. Exploring the Potential of Using Carbonyl Sulfide to Track the Urban Biosphere Signal. *J. Geophys. Res. Atmos.* **126**, e2020JD034106 (2021).
31. Berkelhammer, M. et al. Constraining surface carbon fluxes using in situ measurements of carbonyl sulfide and carbon dioxide. *Global Biogeochem. Cycl.* **28**, 161–179 (2014).
32. Wohlfahrt, G., Hammerle, A., Spielmann, F. M., Kitz, F. & Yi, C. Technical note: Novel estimates of the leaf relative uptake rate of carbonyl sulfide from optimality theory. *Biogeosciences* **20**, 589–596 (2023).
33. Sun, W., Berry, J. A., Yakir, D. & Seibt, U. Leaf relative uptake of carbonyl sulfide to CO_2 seen through the lens of stomatal conductance-photosynthesis coupling. *New Phytol.* **235**, 1729–1742 (2022).
34. Wehr, R. et al. Seasonality of temperate forest photosynthesis and daytime respiration. *Nature* **534**, 680–683 (2016).
35. Järvi, L. et al. Spatial modeling of local-scale biogenic and anthropogenic carbon dioxide emissions in Helsinki. *J. Geophys. Res. Atmos.* **124**, 8363–8384 (2019).
36. Rannik, Ü., Peltola, O. & Mammarella, I. Random uncertainties of flux measurements by the eddy covariance technique. *Atmos. Meas. Tech.* **9**, 5163–5181 (2016).
37. Kohonen, K. M. et al. Towards standardized processing of eddy covariance flux measurements of carbonyl sulfide. *Atmos. Meas. Tech.* **13**, 3957–3975 (2020).
38. Järvi, L. et al. The urban measurement station SMEAR III: continuous monitoring of air pollution and surface-atmosphere interactions in Helsinki, Finland. *Boreal Environ. Res.* **14**, 86–109 (2009).
39. Rebmann, C. et al. ICOS eddy covariance flux-station site setup: a review. *Int. Agrophys.* **10**, 471–494 (2018).
40. Sabbatini, S. et al. Eddy covariance raw data processing for CO_2 and energy fluxes calculation at ICOS ecosystem stations. *Int. Agrophys.* **32**, 495–515 (2018).
41. Aubinet, M., Vesala, T. & Papale, D. (eds) *Eddy Covariance—A Practical Guide to Measurement and Data Analysis* (Springer Atmospheric Sciences, Springer, Dordrecht, 2012).
42. Kooijmans, L. M. J. et al. Canopy uptake dominates nighttime carbonyl sulfide fluxes in a boreal forest. *Atmos. Chem. Phys.* **17**, 11453–11465 (2017).
43. Papale, D. et al. Towards a standardized processing of Net Ecosystem Exchange measured with eddy covariance technique: algorithms and uncertainty estimation. *Biogeosciences* **3**, 571–583 (2006).
44. Aubinet, M. et al. Long term carbon dioxide exchange above a mixed forest in the Belgian Ardennes. *Agric. Forest Meteorol.* **108**, 293–315 (2001).
45. Vekuri, H. et al. A widely-used eddy covariance gap-filling method creates systematic bias in carbon balance estimates. *Sci. Rep.* **13**, 1720 (2023).
46. Kulmala, L. et al. Inter- and intra-annual dynamics of photosynthesis differ between forest floor vegetation and tree canopy in a subarctic Scots pine stand. *Agric. Forest Meteorol.* **271**, 1–11 (2019).
47. Campbell, J. E. et al. Photosynthetic control of atmospheric carbonyl sulfide during the growing season. *Science* **322**, 1085–1088 (2008).
48. Dewar, R. et al. New insights into the covariation of stomatal, mesophyll and hydraulic conductances from optimization models incorporating nonstomatal limitations to photosynthesis. *New Phytol.* **217**, 571–585 (2018).
49. INFRAS, Technical University of Graz (TUG), Institute for Energy and Environment Heidelberg (IFEU), Heinz Steven Data Analysis and Consulting (HSDAC) & WSP Sweden. *Handbook of Emission Factors for Road Transport (HBEFA)* (INFRAS, Technical University of Graz (TUG), Institute for Energy and Environment Heidelberg (IFEU), Heinz Steven Data Analysis and Consulting (HSDAC) & WSP Sweden, 2021).

Acknowledgements

This research has been supported by the Doctoral Program in Atmospheric Sciences (ATM-DP) at the University of Helsinki. For financial support we thank the Research Council of Finland (decisions: 321527 and 325549), the Atmosphere and Climate Competence Center (ACCC, decisions: 3570902 and 357904), the Strategic Research Council working under the Research Council of Finland (decisions: 335201 and 335204) and the European Union's Horizon 2020 Research and Innovation Program under grant agreement No. 101037319. The authors also wish to thank the Finnish Computing Competence Infrastructure (FCCI) for supporting this project with computational and data storage resources. The ChatGPT AI 3.5 language model by OpenAI was used to enhance the language of the manuscript. We thank LUOMUS for allowing us to conduct measurements in their garden. Open access funded by Helsinki University Library.

Author contributions

K.-M.K., P.R., L.K., and L.J. designed research; J.S. and P.R. performed research; H.A. provided auxiliary measurements; J.S. processed and analyzed data; and J.S., K.-M.K., P.R., L.K., H.A., and L.J. wrote the manuscript.

Competing interests

The authors declare no competing interests.

Additional information

Supplementary information The online version contains supplementary material available at https://doi.org/10.1038/s41612-025-00958-5.

Correspondence and requests for materials should be addressed to Jesse Soininen.